Copyright © 2014 Tech Science Press CMES, vol.100, no.1, pp.59-84, 2014

Time Domain Inverse Problems in Nonlinear Systems Using Collocation & Radial Basis Functions

T.A. Elgohary[1], L. Dong[2], J.L. Junkins[3] and S.N. Atluri [4]

Abstract: In this study, we consider ill-posed time-domain inverse problems for dynamical systems with various boundary conditions and unknown controllers. Dynamical systems characterized by a system of second-order nonlinear ordinary differential equations (ODEs) are recast into a system of nonlinear first order ODEs in mixed variables. Radial Basis Functions (RBFs) are assumed as trial functions for the mixed variables in the time domain. A simple collocation method is developed in the time-domain, with Legendre-Gauss-Lobatto nodes as RBF source points as well as collocation points. The duffing optimal control problem with various prescribed initial and final conditions, as well as the orbital transfer Lambert's problem are solved by the proposed RBF collocation method as examples. It is shown that this method is very simple, efficient and very accurate in obtaining the solutions, with an arbitrary solution as the initial guess. Since methods such as the Shooting Method and the Pseudo-spectral Method can be unstable and require an accurate initial guess, the proposed method is advantageous and has promising applications in optimal control and celestial mechanics. The extension of the present study to other optimal control problems, and other orbital transfer problems with perturbations, will be pursued in our future studies.

Keywords: Optimal Control, Inverse Problem, Ill-Posed, Collocation, Radial basis functions.

[1] Department of Aerospace Engineering, Texas A&M University, College Station, TX. Student Fellow, Texas A&M Institute for Advanced Study. Currently a visiting graduate student at University of California, Irvine.

[2] Corresponding author. Department of Engineering Mechanics, Hohai University, China. Email: dong.leiting@gmail.com

[3] Department of Aerospace Engineering, Texas A&M University, College Station, TX. Founding Director, Texas A&M Institute for Advanced Study

[4] Center for Aerospace Research & Education, University of California, Irvine. Also Fellow & Eminent Scholar, Texas A&M Institute for Advanced Study, Texas A&M University, College Station, TX.

1 Introduction

A second-order system of nonlinear ordinary differential equations (ODEs) can, in general, be recast as a system of first-order ODEs in mixed variables [in the sense defined in Atluri (2005); Dong, Alotaibi, Mohiuddine, and Atluri (2014)] as,

$$\dot{\boldsymbol{x}} = \boldsymbol{g}(\boldsymbol{x}, \boldsymbol{f}, t), \qquad t_0 \le t \le t_F \tag{1}$$

where $\boldsymbol{x}$ is the vector of mixed variables, $\boldsymbol{x} \equiv [\boldsymbol{x}_1, \boldsymbol{x}_2]^{\mathrm{T}}$, $\dot{\boldsymbol{x}}_1 = \boldsymbol{x}_2$, $\boldsymbol{f}$ is the force applied to the system, and t is the time with t_0, t_F the initial and final time, respectively. For a specified set of initial conditions $\boldsymbol{x}_0$, and being given the force function $\boldsymbol{f}(t)$, the initial value problem (IVP) of Eq. 1 is well-posed and the solution methodologies are well understood. On the other hand, the inverse problem requiring the solution of the unknown initial conditions, given a prescribed final state, is considered ill-posed. In that sense, Eq. 1 is ill-posed if the full final state vector, $\boldsymbol{x}(t_F)$, is prescribed or, in case of split boundary conditions when both $\boldsymbol{x}_1(t_0)$ and $\boldsymbol{x}_1(t_F)$ are prescribed; or when $\boldsymbol{x}_1(t_0)$ and $\boldsymbol{x}_2(t_F)$ are both prescribed; or when $\boldsymbol{x}_2(t_0)$ and $\boldsymbol{x}_1(t_F)$ are both prescribed; or when $\boldsymbol{x}_2(t_0)$ and $\boldsymbol{x}_2(t_F)$ are both prescribed; or when $\boldsymbol{f}(t)$ is an unknown function to be solved for.

For the majority of applications, $\boldsymbol{f}(t)$ can not be arbitrary and a minimization scheme is introduced to meet a set of engineering requirements. Among those class of problems is the given-time-interval optimal control problem found in several classical works, [Bryson and Ho (1975); Lewis and Syrmos (1995)]. The problem is generally given as,

$$\begin{aligned} &\text{Min:} \quad J = \phi(\boldsymbol{x}(t_F), t_F) + \int_{t_0}^{t_F} L(\boldsymbol{x}, \boldsymbol{f}, t)\mathrm{d}t \\ &\text{Subject to:} \quad \dot{\boldsymbol{x}} = \boldsymbol{g}(\boldsymbol{x}, \boldsymbol{f}, t), \qquad t_0 \le t \le t_F \end{aligned} \tag{2}$$

where the objective is to minimize a prescribed performance index J along the trajectory of the system dynamics given by $\boldsymbol{g}(\boldsymbol{x}, \boldsymbol{f}, t)$. The methodology to obtain the solution for the optimal control force in Eq. 2 is presented in several text books, see [Bryson and Ho (1975); Lewis and Syrmos (1995)] and/or [Lewis, Vrabie, and Syrmos (2012)], based on the calculus of variations, by using Lagrange multipliers to obtain the augmented performance index, J_a:

$$J_a = \phi(\boldsymbol{x}(t_F), t_F) + \int_{t_0}^{t_F} \left\{ L(\boldsymbol{x}, \boldsymbol{f}, t) + \boldsymbol{\lambda}^{\mathrm{T}} [\boldsymbol{g}(\boldsymbol{x}, \boldsymbol{f}, t) - \dot{\boldsymbol{x}}] \right\} \mathrm{d}t \tag{3}$$

The scalar Hamiltonian function is then defined as,

$$H = L(\boldsymbol{x}, \boldsymbol{f}, t) + \boldsymbol{\lambda}^{\mathrm{T}} \boldsymbol{g}(\boldsymbol{x}, \boldsymbol{f}, t) \tag{4}$$

and the augmented performance index can then be re-written as:

$$J_a = \phi(\boldsymbol{x}(t_F), t_F) + \int_{t_0}^{t_F} \left(H - \boldsymbol{\lambda}^{\mathrm{T}}\dot{\boldsymbol{x}}\right)\, \mathrm{d}t \tag{5}$$

The variation of the augmented performance index, δJ_a, is then expressed in terms of the variations of $\boldsymbol{x}$, $\boldsymbol{\lambda}$, and $\boldsymbol{f}$:

$$\begin{aligned}\delta J_a &= \phi_{\boldsymbol{x}}^{\mathrm{T}}\delta\boldsymbol{x}\big|_{t_F} + \int_{t_0}^{t_F} \left[\left(H_{\boldsymbol{x}}^{\mathrm{T}}\delta\boldsymbol{x} - \boldsymbol{\lambda}^{\mathrm{T}}\delta\dot{\boldsymbol{x}}\right) + \left(H_{\boldsymbol{\lambda}}^{\mathrm{T}}\delta\boldsymbol{\lambda} - \dot{\boldsymbol{x}}^{\mathrm{T}}\delta\boldsymbol{\lambda}\right) + H_{\boldsymbol{f}}^{\mathrm{T}}\delta\boldsymbol{f}\right] \\ &= (\phi_{\boldsymbol{x}} - \boldsymbol{\lambda})^{\mathrm{T}}\,\delta\boldsymbol{x}\big|_{t_F} + \boldsymbol{\lambda}^{\mathrm{T}}\delta\boldsymbol{x}\big|_{t_0} \\ &\quad + \int_{t_0}^{t_F} \left[\left(H_{\boldsymbol{x}} + \dot{\boldsymbol{\lambda}}\right)^{\mathrm{T}}\delta\boldsymbol{x} + (H_{\boldsymbol{\lambda}} - \dot{\boldsymbol{x}})^{\mathrm{T}}\,\delta\boldsymbol{\lambda} + H_{\boldsymbol{f}}^{\mathrm{T}}\delta\boldsymbol{f}\right]\mathrm{d}t\end{aligned} \tag{6}$$

where $(\,)_* = \frac{\partial()}{\partial *}$. The stationarity of Eq. 6 necessitates vanishing of $\int_{t_0}^{t_F}[(H_{\boldsymbol{x}} + \dot{\boldsymbol{\lambda}})^{\mathrm{T}}\delta\boldsymbol{x} + (H_{\boldsymbol{\lambda}} - \dot{\boldsymbol{x}})^{\mathrm{T}}\delta\boldsymbol{\lambda} + H_{\boldsymbol{f}}^{\mathrm{T}}\delta\boldsymbol{f}]\mathrm{d}t$, leading to the following 3 Euler-Lagrange equations:

$$\begin{aligned}\dot{\boldsymbol{x}} &= \frac{\partial H}{\partial \boldsymbol{\lambda}} = \boldsymbol{g}(\boldsymbol{x}, \boldsymbol{f}, t) \\ -\dot{\boldsymbol{\lambda}} &= \frac{\partial H}{\partial \boldsymbol{x}} = \frac{\partial L}{\partial \boldsymbol{x}} + \left[\frac{\partial \boldsymbol{g}}{\partial \boldsymbol{x}}\right]^{\mathrm{T}}\boldsymbol{\lambda} \\ \boldsymbol{0} &= \frac{\partial H}{\partial \boldsymbol{f}} = \frac{\partial L}{\partial \boldsymbol{f}} + \left[\frac{\partial \boldsymbol{g}}{\partial \boldsymbol{f}}\right]^{\mathrm{T}}\boldsymbol{\lambda}\end{aligned} \tag{7}$$

And depending on what are prescribed for the states of $\boldsymbol{x}(t_0)$ and $\boldsymbol{x}(t_F)$, some complementary boundary conditions at t_0 and t_F can be obtained from the vanishing of $(\phi_{\boldsymbol{x}} - \boldsymbol{\lambda})^{\mathrm{T}}\,\delta\boldsymbol{x}\big|_{t_F} + \boldsymbol{\lambda}^{\mathrm{T}}\delta\boldsymbol{x}\big|_{t_0}$, as is listed in detail in Tab. 1.

Table 1: Various Cases of Ill-posed Problems Considered in This Study

Prescribed boundary conditions	**Complementary boundary conditions**
$\boldsymbol{x}(t_0)$ prescribed	$\boldsymbol{\lambda}(t_F) = \phi_{\boldsymbol{x}}\big\|_{t_F}$
$\boldsymbol{x}(t_0)$ and $\boldsymbol{x}_1(t_F)$prescribed	$\boldsymbol{\lambda}_2(t_F) = \phi_{\boldsymbol{x}_2}\big\|_{t_F}$
$\boldsymbol{x}_1(t_0)$ and $\boldsymbol{x}_1(t_F)$ prescribed	$\boldsymbol{\lambda}_2(t_0) = \boldsymbol{0}, \boldsymbol{\lambda}_2(t_F) = \phi_{\boldsymbol{x}_2}\big\|_{t_F}$
$\boldsymbol{x}_1(t_0)$ and $\boldsymbol{x}_2(t_F)$ prescribed	$\boldsymbol{\lambda}_2(t_0) = \boldsymbol{0}, \boldsymbol{\lambda}_1(t_F) = \phi_{\boldsymbol{x}_1}\big\|_{t_F}$
$\boldsymbol{x}_2(t_0)$ and $\boldsymbol{x}_1(t_F)$ prescribed	$\boldsymbol{\lambda}_1(t_0) = \boldsymbol{0}, \boldsymbol{\lambda}_2(t_F) = \phi_{\boldsymbol{x}_2}\big\|_{t_F}$

Several solution techniques exist for such problems. The shooting method, see [Press, Teukolsky, Vetterling, and Flannery (2007)], is one of the most widely used

approaches in the optimal control literature. Starting with an initial guess for the unknown initial conditions, the system of equations is integrated and matched with the terminal conditions. By examining the sensitivity, the initial guess is iteratively updated until an acceptable tolerance is achieved at the terminal boundary. The main disadvantage of the shooting method is that a good initial guess is generally required to achieve convergence, which in turn requires the user to have a deep insight of the physical and the mathematical properties of the problem, [von Stryk and Bulirsch (1992)].

By using different trial and test functions, Eq. 7 lends itself to a wide spectrum of solution methodologies [Atluri (2005)], such as collocation, finite volume, Galerkin, MLPG, etc. In [Dong, Alotaibi, Mohiuddine, and Atluri (2014)] a comprehensive review of various computational methods is presented and used to solve well-posed and ill-posed problems of a fourth order ODE describing a beam on an elastic foundation. In [Dai, Schnoor, and Atluri (2012); Dai, Yue, Yuan, and Atluri (2014)], a collocation method with harmonic trial function was developed for studying the nonlinear responses of aeroelastic system. In this study, a simple collocation method is developed, with radial basis functions as trial functions, to tackle various time-domain inverse problems in nonlinear systems. Detailed formulations and numerical examples are given in the following sections.

2 Direct Collocation & Radial Basis Functions

One direct collocation method in optimal control is the pseudo-spectral method. It transforms the set of nonlinear ODEs into a nonlinear programming problem (NLP) by using global polynomials and collocating at Gauss quadrature nodes. The methods were successfully implemented in NASA missions for the International Space Station (ISS) [Kang and Bedrossian (2007)] and the space telescope TRACE [Ross and Karpenko (2012)]. Legendre or Chebyshev polynomials were used as trial functions in [Elnagar, Kazemi, and Razzaghi (1995); Benson, Huntington, Thorvaldsen, and Rao (2006); Fahroo and Ross (2001); Elnagar and Kazemi (1998a)]. Three types of collocations points in the time domain are mostly used: Legendre-Gauss (LG) points, Legendre-Gauss-Radau (LGR) points and Legendre-Gauss-Lobatto (LGL) points. In [Garg, Patterson, Hager, Rao, Benson, and Huntington (2010)], the effect of collocation points on the accuracy of solutions was tested based on a first-order dynamical system. In [Rad, Kazem, and Parand (2012)], radial basis functions (RBFs) were also used as trial functions in a pseudo-spectral frame work. But the solution of the NLP turned out to be very sensitive to the initial guess, and it generally requires one to analytically solve a low order system and provide the solution as the initial guess for the NLP.

In this work, the two-point boundary value problem for an optimal controller is

solved using direct collocation and RBFs without resorting to the pseudo-spectral methods. Using radial basis functions as the trial functions, direct collocation at the LGL nodes leads to a system of nonlinear algebraic equations (NAEs), which are solved using the classical Newton's method. Based on a large number of numerical examples for various time-domain inverse problems, it is shown that the proposed method is very simple, very accurate and insensitive to the initial guess of the unknown states. The detailed formulations are given as follows.

2.1 The Legendre-Gauss-Lobatto (LGL) Nodes

The well known Legendre polynomials are orthogonal to the weight function $w(\tau) = 1$ on the interval $\tau \in [-1,1]$ and satisfy the recursion,

$$\begin{aligned} p_0(\tau) &= 1 \\ p_1(\tau) &= x \\ p_{i+1} &= \left(\frac{2i+1}{i+1}\right)\tau p_i(\tau) - \left(\frac{i}{i+1}\right)p_{i-1}(\tau), \qquad i = 1,2,\ldots \end{aligned} \tag{8}$$

The LGL nodes can then be obtained from solving the differential equation,

$$\left(1-\tau_j^2\right)\dot{p}_N(\tau_j) = 0 \tag{9}$$

which produces the node distribution $-1 = \tau_0 < \tau_1 < \ldots < \tau_N = 1$. The solution of the LGL nodes is generally obtained by numerical algorithms such as in [Elnagar and Kazemi (1998b)]. By a simple mapping in Eq. 10, $\tau = [-1,\ldots,1]$ is transformed into $t = [t_0,\ldots,t_F]$ to obtain the LGL nodes for an arbitrary time interval:

$$t = \frac{t_F - t_0}{2}\tau + \frac{t_F + t_0}{2} \tag{10}$$

2.2 Radial Basis Functions and Collocation

Radial Basis Functions (RBFs) are real-valued functions with values depending on the distance from a source point, $\phi(\boldsymbol{x},\boldsymbol{x}_c) = \phi(\|\boldsymbol{x}-\boldsymbol{x}_c\|) = \phi(r)$. Some of the commonly used types for RBFs are as follows, [Buhmann (2003)]:

$$\begin{aligned} \phi(r) &= e^{-(cr)^2} && \text{Guassian} \\ \phi(r) &= \frac{1}{1+(cr)^2} && \text{Inverse quadratic} \\ \phi(r) &= \sqrt{1+(cr)^2} && \text{Multiquadric} \\ \phi(r) &= \frac{1}{\sqrt{1+(cr)^2}} && \text{Inverse multiquadric} \end{aligned} \tag{11}$$

where $c > 0$ is a shaping parameter.

In this study, the trial functions are expressed for the mixed variables $\boldsymbol{x}_1(t)$ and $\boldsymbol{x}_2(t)$ are both expressed as a linear combination of Gaussian functions, with N LGL nodes $(t_j, j = 1,\ldots,N)$ as the source points, as proposed initially in [Atluri, Han, and Rajendran (2004); Atluri (2005); Dong, Alotaibi, Mohiuddine, and Atluri (2014)]. And the collocation is also performed at the N LGL nodes, leading to:

$$\boldsymbol{x}(t_i) = \sum_{j=0}^{N} \phi(t_i, t_j)\boldsymbol{a}_j, \quad i = 1,\ldots,N \tag{12}$$

In matrix-vector form Eq. 12 can be rewritten as,

$$\boldsymbol{X} = \boldsymbol{\Phi}\boldsymbol{A} \tag{13}$$

where $\boldsymbol{\Phi}$ represents the matrix of basis functions, $\boldsymbol{A}$ is the vector of undetermined coefficients, and $\boldsymbol{X}$ is the vector of unknown states at each LGL node. The time-differentiation of Eq. 13 can be then expressed as,

$$\dot{\boldsymbol{X}} = \dot{\boldsymbol{\Phi}}\boldsymbol{A} \tag{14}$$

Hence, combining Eq. 13 and Eq. 14, $\dot{\boldsymbol{X}}$ is related to $\boldsymbol{X}$ by,

$$\dot{\boldsymbol{X}} = D\boldsymbol{X}, \quad D \equiv \dot{\boldsymbol{\Phi}}\boldsymbol{\Phi}^{-1} \tag{15}$$

where, D is called the derivative matrix, which is generated from the RBFs and their time-derivatives evaluated at the LGL nodes.

Similarly, the co-state functions and its time-derivatives can also be expressed using the same Gaussian functions, leading to:

$$\dot{\boldsymbol{\Lambda}} = D\boldsymbol{\Lambda}, \tag{16}$$

where $\boldsymbol{\Lambda}$ represents the unknown co-states at at each of the LGL nodes.

Using this formulation the state/co-state equations in Eq. 7 and the boundary conditions in Tab. 1 are discretized and transformed into a set of NAEs that can be handled by classical numerical iterative solvers such as Newton's method or by recently-developed Jacobian inverse free methods [Liu and Atluri (2012); Dai, Yue, and Atluri (2014); Elgohary, Dong, Junkins, and Atluri (2014)]. In this study the classical Newton's method is utilized and other Jacobian inverse free NAEs solvers are to be explored in future studies.

3 The Duffing Optimal Control Problem

The duffing equation has been in the literature for almost a century [Cvetićanin (2013)], with a wide range of applications in science and engineering from a nonlinear spring-mass system in mechanics to fault signal detection [Hu and Wen (2003)], and structures design [Suhardjo, Spencer Jr, and Sain (1992)]. The control of a duffing oscillator has a seminal significance to the control problems of nonlinear dynamic responses of structures such as beams, plates, and shells. The duffing oscillator is governed by the following second-order nonlinear ODE:

$$\ddot{x} + \omega_n^2 x + \beta x^3 = f, \quad 0 \le t \le T \tag{17}$$

which can be re-written as a system of 2 first-order ODE equations:

$$\begin{aligned} \dot{x}_1 &= x_2 \\ \dot{x}_2 &= -\omega_n^2 x_1 - \beta x_1^3 + f \end{aligned} \tag{18}$$

where ω_n is the natural frequency and β describes the nonlinearity of the system. With $x_1(0), x_2(0)$ and $f(t)$ being given the problem is well-posed, whereas the ill-posed problem arises from the prescribed: (1) $x_1(T), x_2(T)$; (2) $x_1(0), x_1(T)$; (3) $x_1(0), x_2(T)$; (4) $x_2(0), x_1(T)$; (5) $x_2(0), x_2(T)$, with the unknown forcing function f. In order to satisfy those boundary conditions the force function f is to be obtained subject to a simple performance index :

$$\begin{aligned} \phi(\boldsymbol{x}(t_F), t_F) &= \frac{1}{2}[\boldsymbol{x} - \boldsymbol{x}_F]^{\mathrm{T}} S [\boldsymbol{x} - \boldsymbol{x}_F] \\ L(\boldsymbol{x}, \boldsymbol{f}, t) &= \frac{1}{2}\int_0^T f^2 \mathrm{d}t \end{aligned} \tag{19}$$

Hence,

$$J = \frac{1}{2}[\boldsymbol{x} - \boldsymbol{x}_F]^{\mathrm{T}} S [\boldsymbol{x} - \boldsymbol{x}_F] + \frac{1}{2}\int_0^T f^2 \mathrm{d}t \tag{20}$$

where, $\boldsymbol{x} = [x_1, x_2]^{\mathrm{T}}$, $S > 0$ is assumed diagonal for simplicity, $S \equiv \mathrm{diag}[s_{11}, s_{22}]$, $\boldsymbol{x}_F = [x_{1F}, x_{2F}]^{\mathrm{T}}$ is the desired final state at the specified final time T. The Hamiltonian can then be expressed as,

$$H = \frac{1}{2} f^2 + \lambda_1 x_2 + \lambda_2 \left(-\omega_n^2 x_1 - \beta x_1^3 + f\right) \tag{21}$$

where, λ_1 and λ_2 are the Lagrange multipliers or the system co-states. The necessary conditions that relates the co-states to the controller and minimizes the cost

function are derived from Eq. 7 as,

$$
\begin{aligned}
-\dot{\lambda}_1 &= \frac{\partial H}{\partial x_1} \Rightarrow \dot{\lambda}_1 = \lambda_2\left(\omega_n^2 + 3\beta x_1^2\right) \\
-\dot{\lambda}_2 &= \frac{\partial H}{\partial x_2} \Rightarrow \dot{\lambda}_2 = -\lambda_1 \\
\frac{\partial H}{\partial f} &= 0 \Rightarrow f = -\lambda_2
\end{aligned}
\tag{22}
$$

where different boundary conditions can also be derived following Tab. 1. In this study, several ill-posed problems of the duffing oscillator are considered: the free final state case, the fixed final state case, and the partially prescribed initial & final stated. A simple extension to prescribed periodic solution case is also demonstrated. All these cases are discussed in detail in the following subsections, and are solved by the proposed simple RBF collocation method.

3.1 Free Final State Optimal Control Problem

With prescribed initial conditions $\boldsymbol{x}(0) = [x_{10}, x_{20}]^{\mathrm{T}}$, the objective is to find the optimal forcing function that minimizes the performance index in Eq. 20. From Eq. 6 the boundary conditions imposed on the system of ODEs in Eq. 22 are,

$$
\begin{aligned}
&x_1(0) = x_{10}, \qquad x_2(0) = x_{20} \\
&\lambda_1(T) = s_{11}(x_1(T) - x_{1F}), \qquad \lambda_2(T) = s_{22}(x_2(T) - x_{2F})
\end{aligned}
\tag{23}
$$

where x_{1F}, x_{2F} are the desired final states. Combining Eq. 23 with Eq. 22 and Eq. 18 yields the system of ordinary differential equations with split boundary conditions for the free final state optimal control problem as,

$$
\begin{aligned}
&\left.\begin{aligned}
\dot{x}_1 &= x_2 \\
\dot{x}_2 &= -\omega_n^2 x_1 - \beta x_1^3 - \lambda_2
\end{aligned}\right\} x_1(0), x_2(0) \quad \text{specified} \\
&\left.\begin{aligned}
\dot{\lambda}_1 &= \lambda_2\left(\omega_n^2 + 3\beta x_1^2\right) \\
\dot{\lambda}_2 &= -\lambda_1
\end{aligned}\right\} \begin{aligned}
&\lambda_1(T) = s_{11}(x_1(T) - x_{1F}) \\
&\lambda_2(T) = s_{22}(x_2(T) - x_{2F})
\end{aligned}
\end{aligned}
\tag{24}
$$

Applying RBFs collocation to the system of ODEs in Eq. 24 the total time is divided into N LGL nodes and the system of $4N$ nonlinear algebraic equations is obtained

as,

$$
\begin{aligned}
&R_1^1 = x_1^1 - x_{10} = 0 \\
&R_1^i = Dx_1^i - x_2^i = 0 \\
&R_2^1 = x_2^1 - x_{20} = 0 \\
&R_2^i = Dx_2^i + \omega_n^2 x_1^i + \beta (x_1^i)^3 + \lambda_2^i = 0 \\
&R_3^j = D\lambda_1^j - \lambda_2^j [\omega_n^2 + 3\beta (x_1^j)^2] = 0 \\
&R_3^N = \lambda_1^N - s_{11}(x_1^N - x_{1F}) = 0 \\
&R_4^j = D\lambda_2^j + \lambda_1^j = 0 \\
&R_4^N = \lambda_2^N - s_{22}(x_2^N - x_{2F}) = 0
\end{aligned}
\tag{25}
$$

where, $i = 2, \ldots, N,\ j = 1, \ldots, N-1$. This formulation accommodates the collocation of the boundary conditions without producing an over-determined system of equations [Trefethen (2000)]. The set of $4N$ nonlinear algebraic equations in Eq. 25 can then be solved by the classical Newton's method to obtain the values of the states and the co-states at the collocation nodes.

3.2 Fixed Final State Optimal Control Problem

For this case both the initial and final conditions are prescribed and the optimal forcing function is to be solved for to minimize the general performance index in Eq. 20. The split boundary condition are then given by,

$$
\boldsymbol{x}(0) = \boldsymbol{x}_0, \qquad \boldsymbol{x}(T) = \boldsymbol{x}_F \tag{26}
$$

Applying the necessary conditions in Eq. 7, the optimal control problem can then be formulated as,

$$
\begin{aligned}
&\left.\begin{aligned} \dot{x}_1 &= x_2 \\ \dot{x}_2 &= -\omega_n^2 x_1 - \beta x_1^3 - \lambda_2 \end{aligned}\right\} x_1(0), x_2(0), x_1(T), x_2(T) \quad \text{specified} \\
&\left.\begin{aligned} \dot{\lambda}_1 &= \lambda_2 \left(\omega_n^2 + 3\beta x_1^2\right) \\ \dot{\lambda}_2 &= -\lambda_1 \end{aligned}\right\} \lambda_1, \lambda_2 \quad \text{free}
\end{aligned}
\tag{27}
$$

As in Eq. 25, the system of $4N$ nonlinear algebraic equations is constructed as,

$$\begin{aligned}
&R_1^i = Dx_1^i - x_2^i = 0 \\
&R_2^1 = x_1^1 - x_{10} = 0 \\
&R_2^j = Dx_2^j + \omega_n^2 x_1^j + \beta (x_1^3)^j + \lambda_2^j = 0 \\
&R_2^N = x_1^N - x_{1F} = 0 \\
&R_3^1 = x_2^1 - x_{20} = 0 \\
&R_3^j = D\lambda_1^j - \lambda_2^j (\omega_n^2 + 3\beta (x_1^2)^j = 0 \\
&R_3^N = x_2^N - x_{2F} = 0 \\
&R_4^i = D\lambda_2^i + \lambda_1^i = 0
\end{aligned} \tag{28}$$

where, $i = 1\ldots,N,\ j = 2,\ldots,N-1$. In this way, there are $4N$ nonlinear algebraic equations for $4N$ unknowns.

3.3 Partially Prescribed Initial & Final States

Three additional cases of partially prescribed boundary conditions are formulated in this section. The first case prescribes the initial and final position, $x_1(0), x_1(T)$. The second case prescribes the initial position and final velocity, $x_1(0), x_2(T)$. Finally, the third case prescribes the initial velocity and final position, $x_2(0), x_1(T)$. For each of the three cases the split boundary conditions are derived from Eq. 6 to formulate the ill-posed system of first-order ODEs that is parameterized with RBFs collocation and solved with classical Newton's method. For the first case, the ill-posed set of ODEs is given by,

$$\begin{aligned}
&\left.\begin{aligned}
\dot{x}_1 &= x_2 \\
\dot{x}_2 &= -\omega_n^2 x_1 - \beta x_1^3 - \lambda_2
\end{aligned}\right\} x_1(0), x_1(T) \quad \text{specified} \\
&\left.\begin{aligned}
\dot{\lambda}_1 &= \lambda_2 \left(\omega_n^2 + 3\beta x_1^2\right) \\
\dot{\lambda}_2 &= -\lambda_1
\end{aligned}\right\} \lambda_2(0) = 0,\ \lambda_2(T) = s_{22}(x_2(T) - x_{2F})
\end{aligned} \tag{29}$$

For the second case where initial position and final velocity are prescribed, the set of first-order ODEs with split boundary conditions is given by,

$$\begin{aligned}
&\left.\begin{aligned}
\dot{x}_1 &= x_2 \\
\dot{x}_2 &= -\omega_n^2 x_1 - \beta x_1^3 - \lambda_2
\end{aligned}\right\} x_1(0), x_2(T) \quad \text{specified} \\
&\left.\begin{aligned}
\dot{\lambda}_1 &= \lambda_2 \left(\omega_n^2 + 3\beta x_1^2\right) \\
\dot{\lambda}_2 &= -\lambda_1
\end{aligned}\right\} \lambda_2(0) = 0,\ \lambda_1(T) = s_{11}(x_1(T) - x_{1F})
\end{aligned} \tag{30}$$

Finally, for the case where initial velocity and final position are prescribed, the following equations are obtained,

$$\begin{aligned} &\left.\begin{aligned} \dot{x}_1 &= x_2 \\ \dot{x}_2 &= -\omega_n^2 x_1 - \beta x_1^3 - \lambda_2 \end{aligned}\right\} x_2(0), x_1(T) \quad \text{specified} \\ &\left.\begin{aligned} \dot{\lambda}_1 &= \lambda_2\left(\omega_n^2 + 3\beta x_1^2\right) \\ \dot{\lambda}_2 &= -\lambda_1 \end{aligned}\right\} \lambda_1(0) = 0,\ \lambda_2(T) = s_{22}(x_2(T) - x_{2F}) \end{aligned} \tag{31}$$

For each of these three cases, a collocation scheme which is similar to Eq. 25 and Eq. 28 is used. The only difference is that the boundary conditions at t_0 and t_F are changed to those in Eq. 29, Eq. 30, and Eq. 31.

3.4 Prescribed Harmonic Steady State Achieved by an Optimal Controller

In this case, with a given initial position and velocity, the duffing oscillator is required to achieve a steady harmonic state after a time interval T:

$$\hat{x}(t) = a_1 \cos(\omega t) + a_2 cos(3\omega t) + a_3 \cos(\frac{1}{3}\omega t) \tag{32}$$

where, the frequency, ω, and the amplitudes, a_1, a_2, a_3, are specified, and the same performance index of Eq. 19 is considered.

From Eq. 17, one can see that the controller is defined after T:

$$f = \ddot{\hat{x}} + \omega_n^2 \hat{x} + \beta \hat{x}^3, \quad t \geq T \tag{33}$$

And the solution of the controller between $0 \leq t \leq T$ is entirely equivalent to solve the fixed final state optimal control problem given in section 3.2, with the following fixed final states:

$$\begin{aligned} x_{1F} &= a_1 \cos(\omega T) + a_2 \cos(3\omega T) + a_3 \cos(\frac{1}{3}\omega T) \\ x_{2F} &= -\left[a_1 \omega \sin(\omega T) + 3a_2 \omega \sin(3\omega T) + \frac{1}{3} a_3 \omega \sin(\frac{1}{3}\omega T)\right] \end{aligned} \tag{34}$$

Thus, the same solution procedure given in Eq. 28 is used at here, with RBF as trial functions, and LGL nodes as collocation points.

3.5 Numerical Results

Numerical experiments are conducted for each case of the Duffing optimal control problem in section 3.1-3.4. Tab. 2 shows the parameters used for the numerical simulations. For each case, 40 LGL nodes within the time interval are used as the

RBF source points and collocation points, i.e. $N = 40$. And $c = \frac{N-1}{4T}$ is used for all the examples. the states and the controller resulting from the solution of the NAEs are plotted. And then the obtained initial conditions are fed into a standard numerical integrator, *MATLAB ODE45*. The differences between the solution by collocation and the integrator are plotted at each collocation point, i.e. $\Delta x = x_{RBF} - x_{ODE}$.

Table 2: Duffing Optimal Control Problem Parameters

Parameter	**Value**
Natural frequency, ω_n	1 rad/s
Nonlinearity coefficient, β	≥ 0.9
Initial conditions, $\boldsymbol{x}_0$	$\begin{bmatrix} 0 & 0 \end{bmatrix}^{\mathrm{T}}$
Final conditions, $\boldsymbol{x}_F$	$\begin{bmatrix} 5 & 2 \end{bmatrix}^{\mathrm{T}}$
Harmonic response amplitudes	$a_1 = 1.5, a_2 = 2, a_3 = 3$
Harmonic response frequency	$\omega = 3$ rad/s

For the first case with the free final conditions and $\beta = 0.9$, Fig. 1 shows the states and the controller time history. Fig. 2 shows the errors between the semi-analytic solution obtained by RBFs collocation and the numerical integrator at each collocation point. As shown from the plots, the errors are in the order of $\approx 10^{-7}$ for both the states and the co-states.

The results for the fixed final state case with $\beta = 0.9$ are shown in Fig. 3 for the states and the controller time history. Fig. 4 shows the errors in the states and the co-states. Similar to the free final state case the errors in the states and co-states are very small. It is also worth noting that the shooting method implemented at $\beta \geq 0.9$ will diverge with the arbitrary initial guess used for the RBFs collocation solution.

Fig. 5 and Fig. 6 show the results for the first case of partially prescribed boundary conditions with $x_1(0) = x_{10}$ and $x_1(T) = x_{1F}$. In that case, $\beta = 0.94$. Results for the second case of partial boundary conditions are shown in Fig. 7 and Fig. 8 with $x_1(0) = x_{10}$ and $x_2(T) = x_{2F}$. Similar to the previous case, the same value for the nonlinearity coefficient is chosen. The third case of partial boundary conditions is given by $x_2(0) = x_{20}$ and $x_1(T) = x_{1F}$ with $\beta = 0.97$. Numerical results for this case are shown in Fig. 9 and Fig. 10

Finally, for the case of a prescribed harmonic steady state with $\beta = 0.9$, the results are shown in Fig. 11, whereas the errors in the states and the co-states at each collocation point are shown in Fig. 12(a) and Fig. 12(b), respectively, which is in the order of 10^{-7}

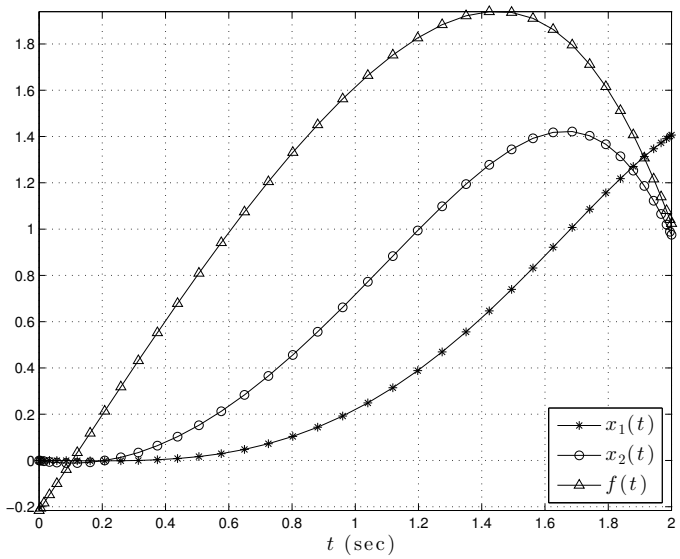

Figure 1: States & Controller, Duffing Free Final State

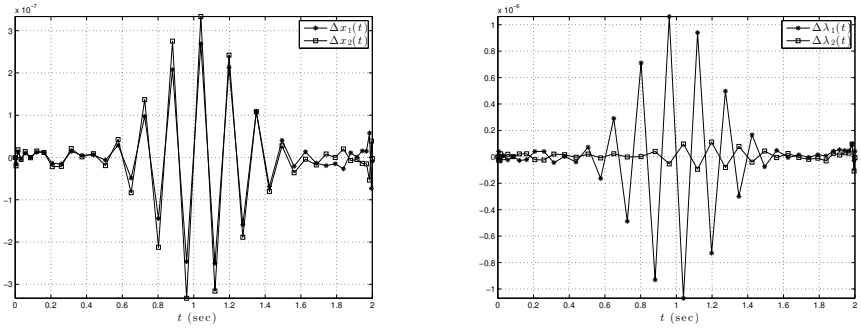

(a) States Error (b) Co-states Error

Figure 2: States & Co-states Errors, Duffing Free Final State

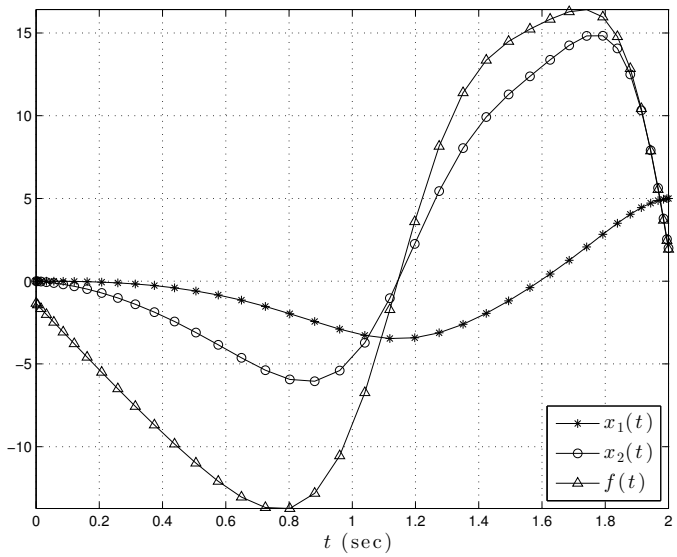

Figure 3: States & Controller, Duffing Fixed Final State

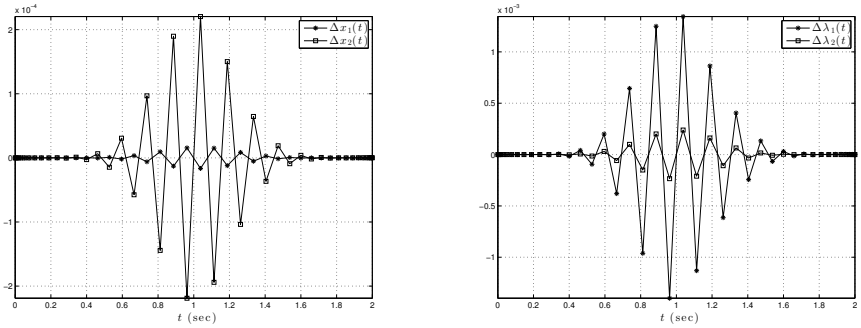

(a) States Error (b) Co-states Error

Figure 4: States & Co-states Errors, Duffing Fixed Final State

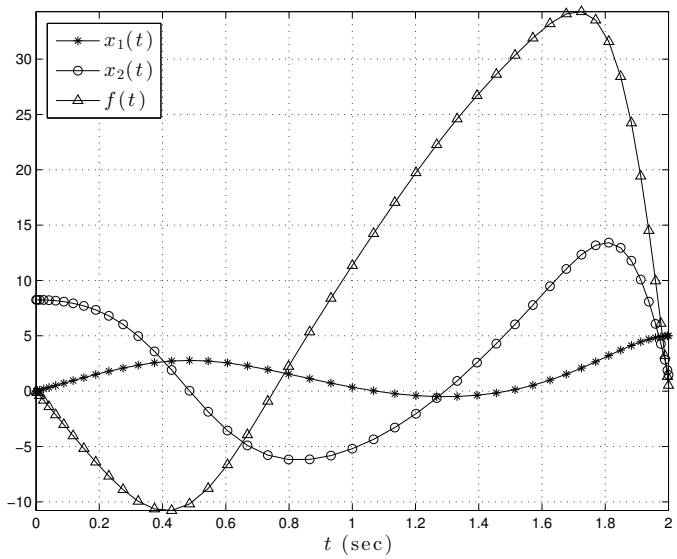

Figure 5: States & Controller, Duffing Prescribed Initial & Final Position

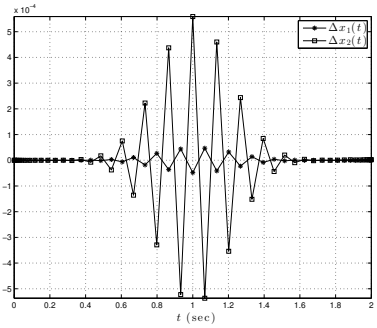

(a) States Error

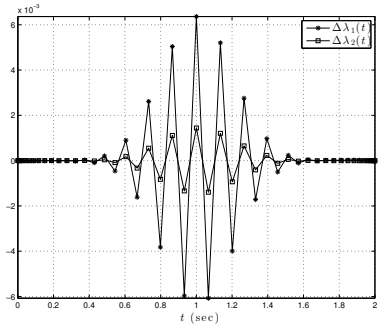

(b) Co-states Error

Figure 6: States & Co-states Errors, Duffing Prescribed Initial & Final Position

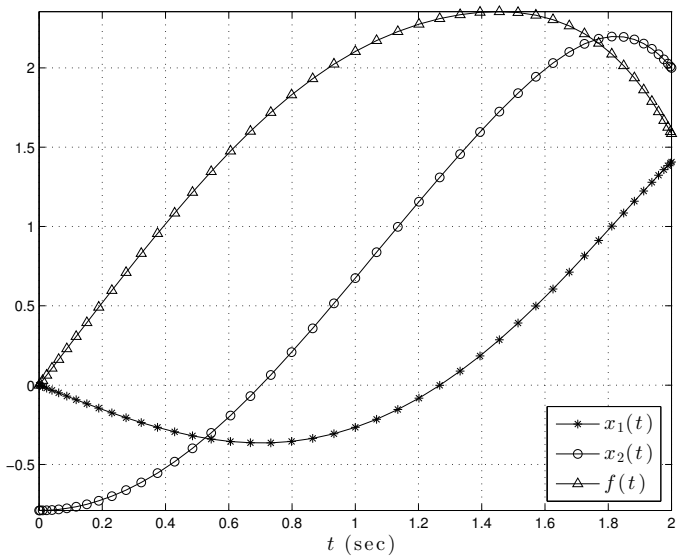

Figure 7: States & Controller, Duffing Prescribed Initial Position & Final Velocity

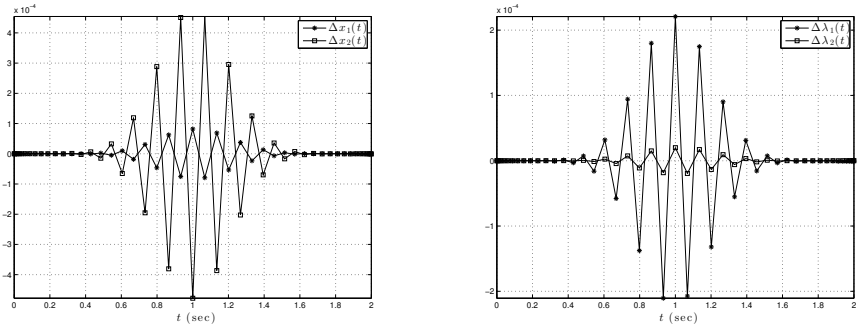

(a) States Error (b) Co-states Error

Figure 8: States & Co-states Errors, Prescribed Initial Position & Final Velocity

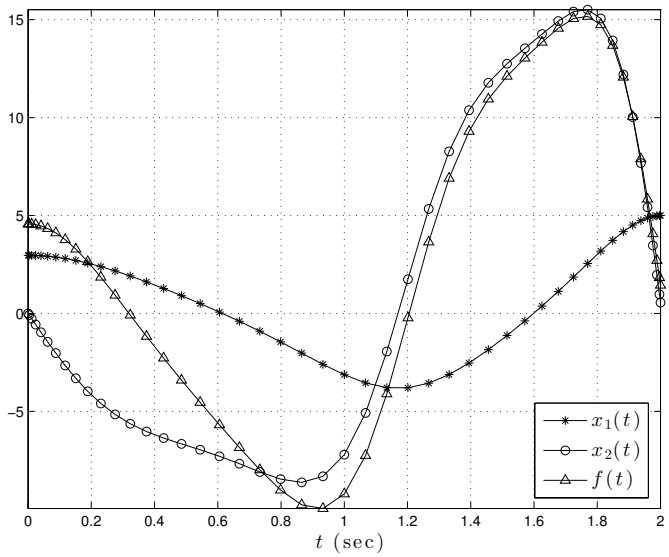

Figure 9: States & Controller, Duffing Prescribed Initial Velocity & Final Position

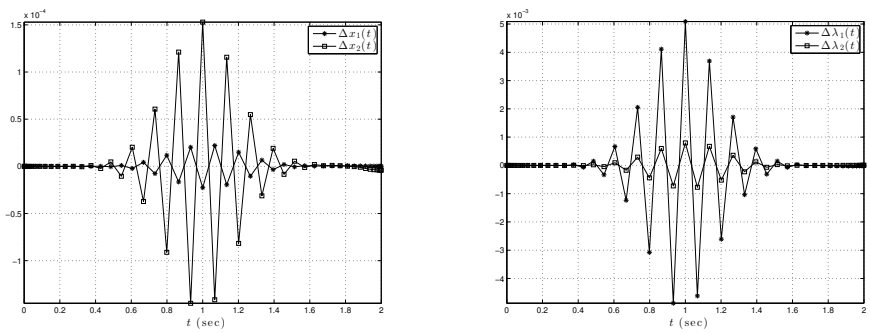

(a) States Error (b) Co-states Error

Figure 10: States & Co-states Errors, Prescribed Initial Velocity & Final Position

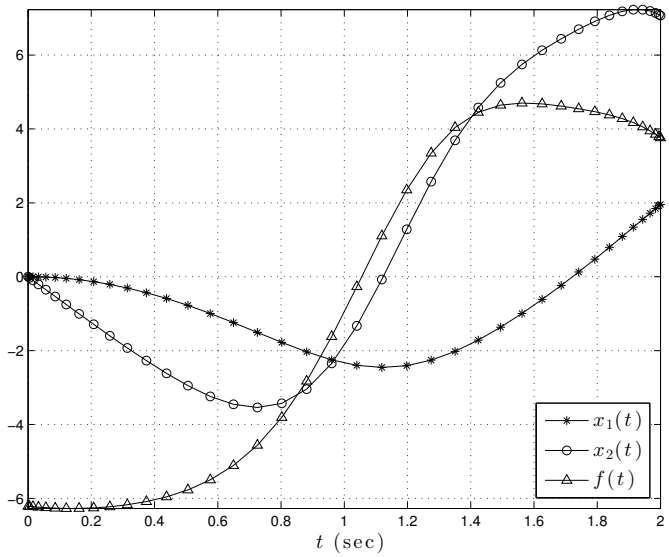

Figure 11: States & Controller, Duffing Prescribed Harmonic State

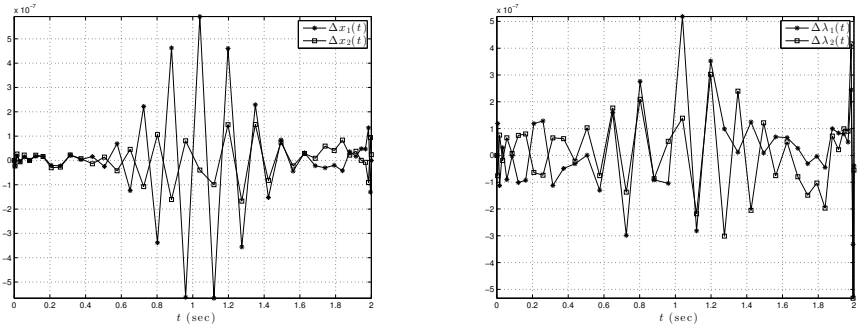

(a) States Error (b) Co-states Error

Figure 12: States & Co-states Errors, Duffing Prescribed Harmonic State

Table 3: Errors in Boundary Conditions

Cases of different BCs	**Error at t_0**	**Error at t_F**
Free final state	$\begin{Bmatrix} 1\times10^{-22} \\ 4.2\times10^{-22} \end{Bmatrix}$	$\begin{Bmatrix} 0 \\ 2.2\times10^{-16} \end{Bmatrix}$
Fixed final state	$\begin{Bmatrix} 9.9\times10^{-18} \\ 0 \end{Bmatrix}$	$\begin{Bmatrix} 1.9\times10^{-17} \\ 0 \end{Bmatrix}$
Prescribed Initial & final position	$\begin{Bmatrix} 3.8\times10^{-17} \\ 6.8\times10^{-19} \end{Bmatrix}$	$\begin{Bmatrix} 0 \\ 1.1\times10^{-16} \end{Bmatrix}$
Prescribed initial position & final Velocity	$\begin{Bmatrix} 6\times10^{-19} \\ 1.4\times10^{-19} \end{Bmatrix}$	$\begin{Bmatrix} 0 \\ 0 \end{Bmatrix}$
Prescribed Initial Velocity & final Position	$\begin{Bmatrix} 3.2\times10^{-17} \\ 3\times10^{-17} \end{Bmatrix}$	$\begin{Bmatrix} 0 \\ 2.2\times10^{-16} \end{Bmatrix}$
Harmonic steady state	$\begin{Bmatrix} 4.3\times10^{-19} \\ 1.4\times10^{-18} \end{Bmatrix}$	$\begin{Bmatrix} 0 \\ 0 \end{Bmatrix}$

Tab. 3 shows the errors between the prescribed boundary conditioned and the ones obtained from solving the set of nonlinear algebraic equations. It is shown that the discretization of the fixed time-interval optimal control problem using RBFs as trial functions, and simple collocation at the LGL nodes, has demonstrated its high accuracy for all cases of boundary conditions explored in this study.

4 Orbital Transfer Two-point Boundary Value Problem

Another classical problem in celestial mechanics is the two-point boundary value problem of orbital transfer. This problem is known as Lambert's problem after Johann Heinrich Lambert (1728–1779) who was the first to state and to solve the problem. The objective is to find the transfer orbit that connects two points in space given a flight time. Fig. 13 illustrates the geometry of Lambert's problem with $t_0, \boldsymbol{r}_0$ the initial time and position, $t_F, \boldsymbol{r}_F$ the desired final time and position, $\boldsymbol{v}_0$ the initial velocity to be solved for that would generate the transfer orbit and $\boldsymbol{v}_F$ the terminal velocity at the desired position.

The dynamics of the unperturbed relative two-body problem is obtained from New-

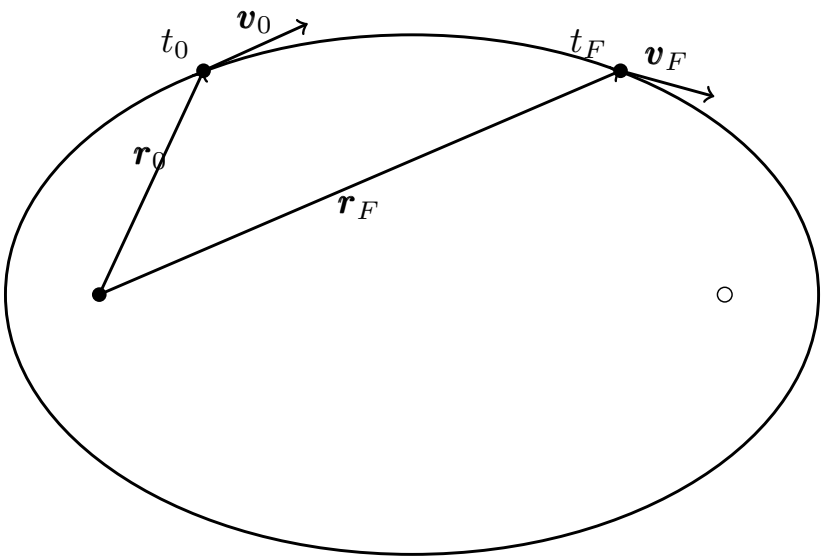

Figure 13: Illustration of the Orbital Transfer Problem

ton's famous universal gravitational law as,

$$\ddot{\boldsymbol{r}} = \frac{-\mu}{r^3}\boldsymbol{r} \tag{35}$$

where, $\boldsymbol{r} = \begin{bmatrix} x & y & z \end{bmatrix}^{\mathrm{T}}$ is the position vector in the inertial frame, μ is the Earth gravitational parameter $\mu \approx 3.986 \times 10^{14}$ m^{3}s^{-2} and $r = \sqrt{x^2+y^2+z^2}$.

Solving the unperturbed Lambert's problem analytically was discussed in detail in [Battin (1999)]. The solution developed still has a singularity for transfer angles of $\pm 180°$. In [Schaub and Junkins (2003)], a numerical iterative method is introduced to handle both singularities and gravitational perturbations in Lambert's problem. The method is essentially a shooting algorithm where a sufficiently good initial guess for the initial velocity is needed to improve convergence. Generally, the initial guess for the velocity vector is obtained such that the target position is reached but not necessarily in the required transfer time. The present solution based on RBFs collocation starts with an arbitrary initial guess, and can readily handle any perturbations to provide a semi-analytic solution for the transfer orbit problem.

As a first order system of equations the unperturbed two-body problem is written

as,

$$
\begin{aligned}
\dot{x}_1 &= x_2 \\
\dot{x}_2 &= \frac{-\mu}{r^3} x_1 \\
\dot{y}_1 &= y_2 \\
\dot{y}_2 &= \frac{-\mu}{r^3} y_1 \\
\dot{z}_1 &= z_2 \\
\dot{z}_2 &= \frac{-\mu}{r^3} z_1
\end{aligned}
\tag{36}
$$

The RBFs collocation can then be applied to Eq. 36 to produce a set of $6N$ nonlinear algebraic equations where N is the number of LGL collocation nodes:

$$
\begin{aligned}
R_1^i &= Dx_1^i - x_2^i = 0 \\
R_2^i &= Dy_1^i - y_2^i = 0 \\
R_3^i &= Dz_1^i - z_2^i = 0 \\
R_4^1 &= x_1^1 - x_{10} = 0 \\
R_4^j &= Dx_2^j + \frac{\mu}{r^j} x_1^j = 0 \\
R_4^N &= x_1^N - x_{1F} = 0 \\
R_5^1 &= y_1^1 - y_{10} = 0 \\
R_5^j &= Dy_2^j + \frac{\mu}{r^j} y_1^j = 0 \\
R_5^N &= y_1^N - y_{1F} = 0 \\
R_6^1 &= z_1^1 - z_{10} = 0 \\
R_6^j &= Dz_2^j + \frac{\mu}{r^j} z_1^j = 0 \\
R_6^N &= z_1^N - z_{1F} = 0
\end{aligned}
\tag{37}
$$

where, $i = 1, \ldots, N$ and $j = 2, \ldots, N-1$ which produces a system of $6N$ equations in $6N$ unknowns. As a numerical example an orbit is examined with initial and final position given by,

$$
\begin{aligned}
\boldsymbol{r}_0 &= \begin{bmatrix} 2.87 & 5.19 & 2.85 \end{bmatrix}^{\mathrm{T}} \times 10^6\,\mathrm{m} \\
\boldsymbol{r}_F &= \begin{bmatrix} 2.09 & 7.82 & 0 \end{bmatrix}^{\mathrm{T}} \times 10^6\,\mathrm{m}
\end{aligned}
\tag{38}
$$

The transfer time is chosen to be $t_F = 0.05$ days or $t_F = 4.32 \times 10^3$ seconds. The number of LGL nodes is set as, $N = 47$, with the shaping parameter, $c = \frac{N+3}{4T}$.

The set of nonlinear algebraic equations in Eq. 37 is solved with an arbitrary initial guess. And the resulting orbit is compared against the closed form Lagrange/Gibbs (F& G) solution, [Battin (1999); Schaub and Junkins (2003)], considering the initial position and velocity vector obtained from the RBFs collocation method. The resulting position and velocity are compared in Fig. 14 and Fig. 15, respectively.

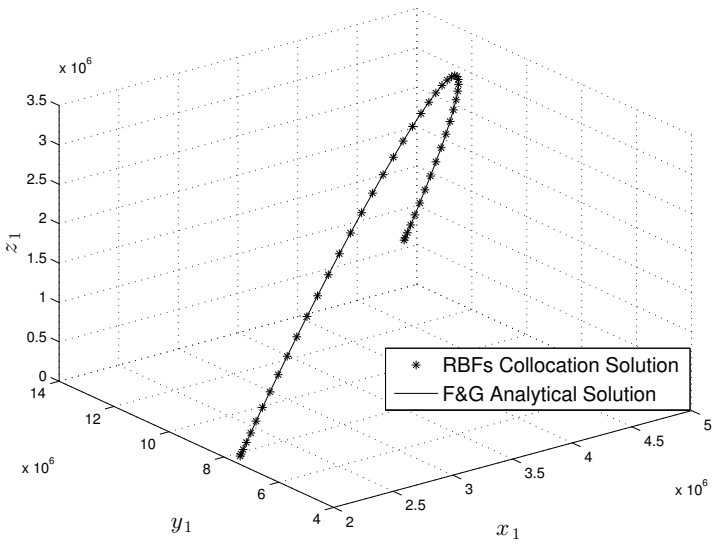

Figure 14: Transfer Orbit Position Propagation

Table 4: Errors in Boundary Conditions

Initial Boundary Error	**Terminal Boundary Error**
$\begin{Bmatrix} 0 \\ 0 \\ 0 \end{Bmatrix}$ m	$\begin{Bmatrix} 9.610^{-3} \\ 16.3 \times 10^{-3} \\ 10.2 \times 10^{-3} \end{Bmatrix}$ m

The errors of the initial and the terminal boundary conditions are compared as in Tab. 3 in Tab. 4. The initial conditions obtained by the RBF collocation method drives the object to the desired final position with millimeter accuracy. This approach using RBFs collocation thus is quite advantageous compared to previous analytical and numerical methods of solving the Lambert's problem. And it can be

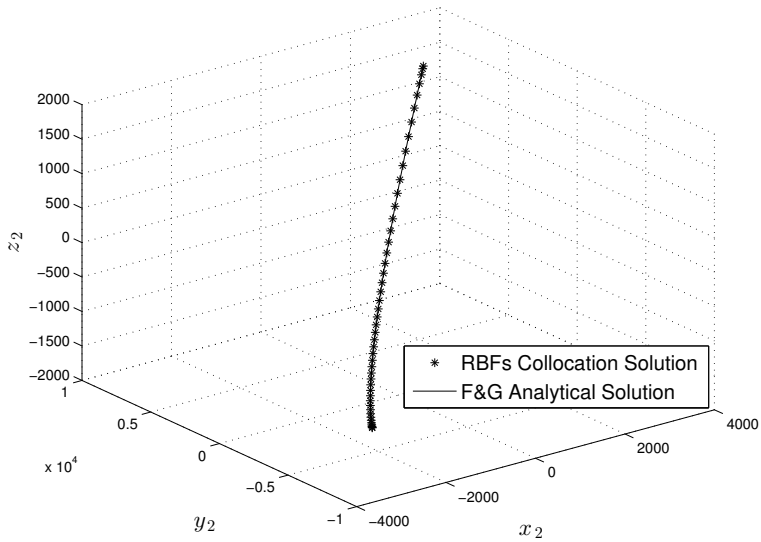

Figure 15: Transfer Orbit Velocity Propagation

extended in future to to address perturbations and obtain what is known as pork-chop plots for the selection of launch and arrival times while minimizing fuel or some other specified parameters.

5 Conclusion

The present simple collocation scheme based on radial basis functions and LGL collocation points is proven to be very accurate and efficient in solving time domain inverse problems. Starting with the Duffing OCP, all the cases considered achieved very high accuracy in the initial and final conditions. The solution is insensitive to the initial guess and does not require any insight into the physics of the problem. Several extensions are possible for the OCP to include intermediate boundary conditions or inequality constraints along the trajectory. The orbital transfer problem based on the same formulation achieved millimeter accuracy when compared to the analytical Lagrange/Gibbs F&G solution. Unlike the shooting method which requires the problem to be solved first for an arbitrary time and the solution to fed in as the initial guess, the RBFs collocation approach started at an arbitrary set of initial conditions and achieved very high accuracy in determining the transfer orbit. The method can be utilized to provide pork-chop plots for launch and arrival times

for mission design. For all the cases considered in this work, the generated set of NAEs are solved with the classical Newton's method whereas several Jacobian inverse free methods exist and can be explored in future studies, [Liu and Atluri (2012); Dai, Yue, and Atluri (2014); Elgohary, Dong, Junkins, and Atluri (2014)].

Acknowledgement: This work is supported by the US Army Research Labs VT Division, under an AFRL / UCI collaborative research agreement. The encouragement of Messrs. Dy Le and Jarret Riddick is thankfully acknowledged. This work is also supported by the Texas A&M Institute for Advanced Study (TIAS). It was initiated while S.N. Atluri visited TIAS briefly in January, 2014.

References

Atluri, S. N. (2005): *Methods of computer modeling in engineering & the sciences*, volume 1. Tech Science Press Palmdale.

Atluri, S. N.; Han, Z. D.; Rajendran, A. M. (2004): A new implementation of the meshless finite volume method, through the mlpg "mixed" approach. *Computer Modeling in Engineering and Sciences*, vol. 6, no. 6, pp. 491–514.

Battin, R. H. (1999): *An introduction to the mathematics and methods of astrodynamics*. AIAA.

Benson, D. A.; Huntington, G. T.; Thorvaldsen, T. P.; Rao, A. V. (2006): Direct trajectory optimization and costate estimation via an orthogonal collocation method. *Journal of Guidance, Control, and Dynamics*, vol. 29, no. 6, pp. 1435–1440.

Bryson, A. E.; Ho, Y.-C. (1975): *Applied optimal control: optimization, estimation and control*. CRC Press.

Buhmann, M. D. (2003): *Radial basis functions: theory and implementations*, volume 5. Cambridge university press Cambridge.

Cvetićanin, L. (2013): Ninety years of duffing's equation. *Theoretical and Applied Mechanics*, vol. 40, no. 1, pp. 49–63.

Dai, H.; Yue, X.; Atluri, S. (2014): Solutions of the von kármán plate equations by a galerkin method, without inverting the tangent stiffness matrix. *Journal of Mechanics of Materials and Structures*, vol. 9, no. 2, pp. 195–226.

Dai, H.; Yue, X.; Yuan, J.; Atluri, S. N. (2014): A time domain collocation method for studying the aeroelasticity of a two dimensional airfoil with a structural nonlinearity. *Journal of Computational Physics*, vol. 270, pp. 214–237.

Dai, H.-H.; Schnoor, M.; Atluri, S. N. (2012): A simple collocation scheme for obtaining the periodic solutions of the duffing equation, and its equivalence to the

high dimensional harmonic balance method: subharmonic oscillations. *Computer Modeling in Engineering and Sciences*, vol. 84, no. 5, pp. 459–497.

Dong, L.; Alotaibi, A.; Mohiuddine, S.; Atluri, S. (2014): Computational methods in engineering: a variety of primal & mixed methods, with global & local interpolations, for well-posed or ill-posed bcs. *CMES: Computer Modeling in Engineering & Sciences*, vol. 99, no. 1, pp. 1–85.

Elgohary, T. A.; Dong, L.; Junkins, J. L.; Atluri, S. N. (2014): Solution of post-buckling & limit load problems, without inverting the tangent stiffness matrix & without using arc-length methods. *CMES: Computer Modeling in Engineering & Sciences*, vol. 98, no. 6, pp. 543–563.

Elnagar, G.; Kazemi, M. A.; Razzaghi, M. (1995): The pseudospectral legendre method for discretizing optimal control problems. *Automatic Control, IEEE Transactions on*, vol. 40, no. 10, pp. 1793–1796.

Elnagar, G. N.; Kazemi, M. A. (1998): Pseudospectral chebyshev optimal control of constrained nonlinear dynamical systems. *Computational Optimization and Applications*, vol. 11, no. 2, pp. 195–217.

Elnagar, G. N.; Kazemi, M. A. (1998): Pseudospectral legendre-based optimal computation of nonlinear constrained variational problems. *Journal of computational and applied mathematics*, vol. 88, no. 2, pp. 363–375.

Fahroo, F.; Ross, I. M. (2001): Costate estimation by a legendre pseudospectral method. *Journal of Guidance, Control, and Dynamics*, vol. 24, no. 2, pp. 270–277.

Garg, D.; Patterson, M.; Hager, W. W.; Rao, A. V.; Benson, D. A.; Huntington, G. T. (2010): A unified framework for the numerical solution of optimal control problems using pseudospectral methods. *Automatica*, vol. 46, no. 11, pp. 1843–1851.

Hu, N.; Wen, X. (2003): The application of duffing oscillator in characteristic signal detection of early fault. *Journal of Sound and Vibration*, vol. 268, no. 5, pp. 917–931.

Kang, W.; Bedrossian, N. (2007): Pseudospectral optimal control theory makes debut flight, saves nasa $ 1 m in. *SIAM news*, vol. 40, no. 7.

Lewis, F. L.; Syrmos, V. L. (1995): *Optimal Control*. Wiley, New York.

Lewis, F. L.; Vrabie, D.; Syrmos, V. L. (2012): *Optimal control*. John Wiley & Sons.

Liu, C.-S.; Atluri, S. N. (2012): A globally optimal iterative algorithm using the best descent vector x= λ [αcf+ bt f], with the critical value αc, for solving a system

of nonlinear algebraic equations f (x)= 0. *Computer Modeling in Engineering and Sciences*, vol. 84, no. 6, pp. 575.

Press, W. H.; Teukolsky, S. A.; Vetterling, W. T.; Flannery, B. P. (2007): *Numerical recipes 3rd edition: The art of scientific computing*. Cambridge university press.

Rad, J.; Kazem, S.; Parand, K. (2012): A numerical solution of the nonlinear controlled duffing oscillator by radial basis functions. *Computers & Mathematics with Applications*, vol. 64, no. 6, pp. 2049–2065.

Ross, I. M.; Karpenko, M. (2012): A review of pseudospectral optimal control: From theory to flight. *Annual Reviews in Control*, vol. 36, no. 2, pp. 182–197.

Schaub, H.; Junkins, J. L. (2003): *Analytical mechanics of space systems*. AIAA.

Suhardjo, J.; Spencer Jr, B.; Sain, M. (1992): Non-linear optimal control of a duffing system. *International journal of non-linear mechanics*, vol. 27, no. 2, pp. 157–172.

Trefethen, L. N. (2000): *Spectral methods in MATLAB*, volume 10. SIAM.

von Stryk, O.; Bulirsch, R. (1992): Direct and indirect methods for trajectory optimization. *Annals of operations research*, vol. 37, no. 1, pp. 357–373.